Aromaticity of pericyclic reaction transition structures: magnetic evidence

Haijun Jiao and Paul von Ragué Schleyer*

Computer-Chemistry-Center, Institut für Organische Chemie, Universität Erlangen-Nürnberg, Henkestrasse 42, 91054 Erlangen, Germany

ABSTRACT: The transition states of thermally allowed pericyclic reactions are aromatic. They not only have highly delocalized structures and large resonance stabilizations (energies of concert), but also strongly enhanced magnetic susceptibilities (Λ) and appreciable NICS (nucleus-independent chemical shifts) values arising from the diatropic ring currents. Aromaticity is the consequence of cyclic electron delocalization, which can have σ and hybrid, and not just π character. © 1998 John Wiley & Sons, Ltd.

KEYWORDS: pericyclic reaction transition structures; aromaticity; magnetic susceptibility

INTRODUCTION

The analogy between the π electrons of benzene and the six delocalized electrons in the cyclic transition state of the Diels–Alder reaction of butadiene and ethylene was recognized by Evans and Warhurst in 1938.[1] Regarding the relationship between stability and reactivity, they observed that 'conjugated molecules show on the one hand enhanced thermochemical stability, while on the other hand they show in some of their reactions greater reactivity than do non-conjugated substances.' Evans[2] also pointed out that 'the greater the mobility of the π electrons in the transition state the greater will be the lowering of the activation energy.'

Generalized through the Woodward–Hoffmann rules[3] and the Hückel–Möbius concept by Zimmerman,[4] thermally allowed pericyclic reactions are considered to take place preferentially through concerted aromatic transition states which are favored energetically.[5] In addition to the qualitative MO theories, detailed quantitative analysis of the structures and energies of the pericyclic transition states have been carried out with semiempirical methods,[6] at increasingly high *ab initio* levels[7,8] and by using density functional theory.[9]

The aromaticity of pericyclic transition states has been analyzed systematically by Jiao and Schleyer[8] on the basis of the geometric, energetic and magnetic criteria. In addition to the geometric and energetic evidence that aromatic transition states have delocalized structures and large resonance stabilization (energies of concert[10]), they

found that such transition structures exhibit strongly enhanced magnetic susceptibilities and susceptibility anisotropies as well as abnormal ^{1}H chemical shifts.

As a further development, Schleyer *et al.*[11] have proposed recently the use of the negative of the computed magnetic shieldings at or above the ring center, referred to as 'nucleus-independent chemical shifts' (NICS), as a simple and effective criterion for aromaticity. NICS, as an indicator of aromaticity, agrees well with the energetic, geometric, and magnetic criteria, and does not require increment systems for other references. In a concurrent study, NICS is also an effective probe of the individual rings in polycyclic systems.[12] Most recently, Lecea *et al.*[13] used NICS to characterize the in-plane aromaticity of 1,3-dipolar cycloaddition transition states, and only found evidence for the in-plane delocalization; the π (out-of plane) effects are negligible.

We have now employed the computed energetic, geometric properties and especially magnetic susceptibility enhancements (Λ) and NICS to characterize the aromaticity of several pericyclic transition states: (a) acetylene trimerization to benzene; (b) isomerization from diademane to triquinacene; and (c) some typical aromatic transition states.

COMPUTATIONAL METHODS

Geometry optimizations and frequency calculations were carried out at HF/6–31G*, RMP2/6–31G* *ab initio* and at B3LYP/6–311 + G** density functional levels (for uniform comparisons) using the Gaussian 94 program.[14] The magnetic susceptibilities χ_{tot} were calculated with the IGLO method using the recommended DZ and II basis sets.[15] The magnetic susceptibility enhancement (Λ) for

the transition structure was defined as the increase in magnetic susceptibility from the reactants to the transition state. The NICS values at the geometrical centers of interest were calculated at the GIAO-SCF/6–31G* level with B3LYP/6–311 + G** geometries using the Gaussian 94 program.

For the acetylene trimerization, we examined the changes in NICS along the reaction coordinate. As a refinement, we employed not only the NICS(tot) but also the separated NICS(π) and NICS(σ) contributions to characterize the ring current effects. These calculations were carried out at the SOS-DFPT-IGLO level using the Perdew–Wang-91 exchange-correlation functional and the IGLO-III TZ2P basis set. The Pipek and Mezey localization procedure used to separate the σ and π components of double bonds[16] was implemented by Malkin et al. in the DeMon–Master program.[17]

RESULTS AND DISCUSSION

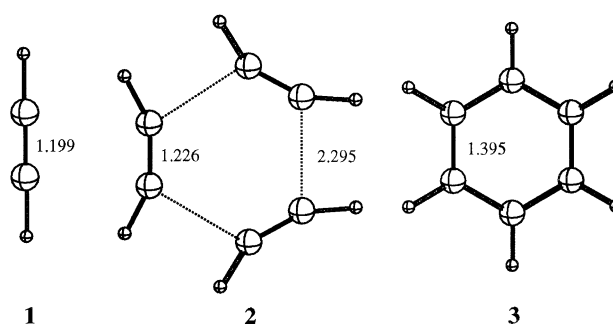### Trimerization of acetylene to benzene

Although the energetic advantages of aromatic delocalization in cyclic transition states are well known, even thermally allowed and strongly exothermic reactions may have substantial activation barriers. One example is the trimerization of acetylene to benzene. Based on the experimental heats of formation of benzene and acetylene, this trimerization is extremely exothermic, 143 kcal mol^{-1} (1 kcal = 4.184 kJ).[18] Although no experimental activation energy is known, the barrier can be computed easily. For example, Houk et al.[18] pointed out that 60 kcal mol^{-1} of the 80 kcal mol^{-1} barrier at STO-3G is due to the energy required to distort the three acetylenes to the transition state geometry. The remaining 20 kcal mol^{-1} must arise mainly from the electronic interactions. In a similar study, Bach et al.[19] found that the electronic contribution to the barrier (which is lower, 62 kcal mol^{-1} at MP3/6–31G*) is dominated by the closed-shell repulsions between filled orbitals and concluded that there is no π-aromatic stabilization in this six-electron pericyclic transition state. Nevertheless, this transition state still be aromatic, but how can this be demonstrated?

As shown in Fig. 1, the potential energy surface along the HF/6–31G* intrinsic reaction coordinate (IRC) is flat from the three acetylene reactants to the transition state, but very steep after the transition state to benzene. Furthermore, this process is concerted and synchronous.

At B3LYP/6–311 + G**, a D_{3h} symmetrical structure is the authentic transition state with a single imaginary frequency (-653 cm^{-1}) and C—C separations of 1.226 and 2.295 Å (Fig. 2). The calculated reaction enthalpy is exothermic by 139.5 kcal mol^{-1} at B3LYP/6–311 + G**+ ZPE (B3LYP/6–311 + G**) (this is close to the experimental value of 143 kcal mol^{-1}). The B3LYP
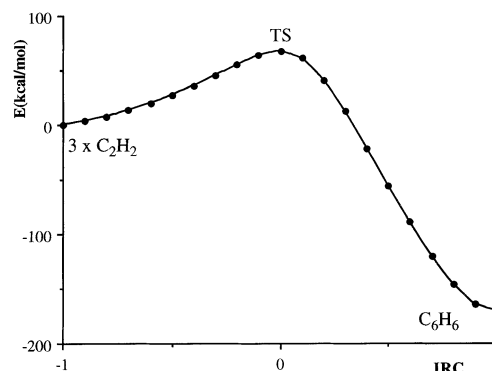
Figure 1. Relative energies of acetylene trimerization along the HF/6–31G* intrinsic reaction coordinate (IRC, compare with Fig. 3)

Figure 2. B3LYP/6–311 + G** geometries for acetylene (**1**), the trimerization transition state (**2**) and benzene (**3**)

Table 1. B3LYP/6–311 + G** total energies (hartree) zero-point energies (ZPE, kcal mol^{-1}) relative energies (kcal mol^{-1}) and magnetic susceptibilities (χ_{tot}, ppm cgs) for the acetylene trimerization reaction

Parameter	3 C$_2$H$_2$	TS	Benzene
E_{tot}[a]	-232.06995[b]	-231.99227	-232.31130
ZPE	50.9	52.5	62.8
MP4/6–311G*[c]	-231.36891	-231.29374	-231.61033
E_{rel}[d]	0.0	50.3[e]	-139.5[f]
E_{rel}(MP4)[g]	0.0	48.8[e]	-139.6[f]
χ_{tot}	-74.4	-88.5	-68.0
$\Delta_{\chi_{tot}}$	0.0	-14.1	6.4

[a] At B3LYP/6–311 + G**.
[b] -77.33802 au for a distorted acetylene moiety with the same geometry as in the transition state.
[c] Single-point energies at MP4SDTQ/6–311G*//MP2/6–31G*.
[d] At B3LYP/6–311 + G** + ZPE (B3LYP/6–311 + G**).
[e] Activation energy.
[f] Reaction enthalpy.
[g] MP4SDTQ/6–311G*//MP2/6–31G* + ZPE (B3LYP/6–311 + G**).
[h] IGLO/II//B3LYP/6–311 + G**.

computed barrier of 50.3 kcal mol^{-1} agrees well with the highly correlated MP4SDTQ/6–311G* result of 48.8 kcal mol^{-1} (Table 1). To estimate the acetylene distortion in the transition state, single-point calculations on the deformed acetylene geometry give a total strain

energy of 35.1 kcal mol^{-1}. This is 70% of the activation barrier.

In order to assess the aromaticity of the transition state, we calculated its magnetic susceptibility exaltation (Λ, a property directly associated with aromaticity).[8,11,12,20,21] Owing to ring current effects, aromatic systems show magnetic susceptibility enhancements (more negative values of χ_M than those expected from the group increment additivity). In the acetylene trimerization, the enhancement (Λ) is defined as the difference in magnetic susceptibility between the transition state and the sum of three acetylenes. At IGLO/II//B3LYP/6–311 + G**, the calculated Λ of -14.6 ppm cgs (Table 1), comparable to the benzene value of -13.4 ppm cgs, indicates its aromatic character. This agrees well with Λ values of the other aromatic transition states with six delocalized electrons.[8]

In addition to Λ, the change of the NICS values along the HF/6–31G* intrinsic reaction coordinate (IRC) also was explored. Not only the total value, NICS(tot), but also the separated NICS(π) and NICS(σ) components were computed with the DeMon–Master program. As shown in Fig. 3, diamagnetic NICS(tot) has a maximum at the transition state geometry and the change in the diamagnetic NICS(π) is small in the beginning of the reaction, and varies considerably only past the transition state. On the other hand, NICS(σ) is highly diamagnetic at the transition state, but strongly paramagnetic in benzene and zero for three separated acetylenes. The relatively small NICS(tot) for benzene is due to the diamagnetic NICS(π) and paramagnetic NICS(σ) compensation (Fig. 3). In the transition state, the large NICS(σ) of -13.5 ppm is 56% of the NICS(tot) value; this indicates that the in-plane contribution is larger, but the out-of-plane π delocalization is also important.

Isomerization between diademane and triquinacene

Prepared by Woodward *et al.*[22] in 1964, triquinacene (**4**) with three C=C double bonds in rigid positions has been considered controversially as a possible neutral homoaromatic compound. Spectroscopic studies[22] and the X-ray structure[23] indicated **4** not to be homoaromatic. The homoaromaticity of **4** based on the stepwise heats of hydrogenation[24] has not been confirmed by force field, semiempirical (AM1) and *ab initio* computations as well as by a combined experimental and DFT study.[25d] In this paper, the enthalpy of formation of triquinacene has been determined both experimentally by measuring the heat of combustion in a microcalorimeter and computationally at a high level of density functional theory. Since the enthalpy of formation of triquinacene is about 4 kcal/mol higher than the value reported by Liebman *et al.*,[25] the previously deduced homoaromatic stabilization (claimed
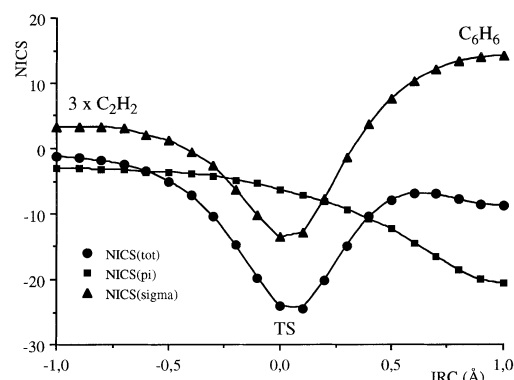
Figure 3. SOS-DFPT-PW91/III//HF/6–31G* calculated NICS(tot), NICS(π) and NICS(σ) along the HF/6–31G* IRC (see Fig. 1): IRC = -1 for three acetylene with C—C separations of 3.052 Å; IRC = 0 for transition state and IRC = 1 for benzene with a C—C bond length of 1.386 Å. The core and C—H contributions are not given

to be 4.5 kcal/mol) is not present. Triquinacene is not a neutral homoaromatic molecule.

As shown in Figure 4, our B3LYP/6–311 + G** and MP2/6–31G* C—C single bond lengths agree very well with the X-ray results,[23] but the computed C=C double bond lengths, 1.342 and 1.333 Å, are longer than the questionably too short experimental value of 1.319 Å.

In addition to extensive energetic analysis, our magnetic evidence for the non-homoaromaticity of **4** is based on Λ and NICS values. We employed the increment system[26] to estimate the Λ of **4**. Generally, Λ is defined as the difference between the bulk magnetic susceptibility (χ_M) of a compound and the susceptibility (χ_M) estimated from an additivity scheme for the same structure, assuming no cyclic delocalization ($\Lambda = \chi_M - \chi_M$). Since magnetic susceptibilities of non-aromatic organic molecules show additive behavior of their constituent groups, values of χ_M can be estimated within an accuracy of a few ppm cgs by increment methods based on group (e.g. CH_3, CH_2, CH and C) contributions.

There are four methine (>CH—) groups and three *cis* —HC=CH— units in **4**. At IGLO/DZ/MP2/6–31G*, the Λ of **4** has been computed to be -0.2 ppm cgs; this indicates that **4** is definitively not homoaromatic. The same conclusion is deduced from the negligible NICS (-2.7 ppm) calculated at the geometric center equally distant from the three C=C double bonds.

In contrast, the isomerization transition state (**5**) from diademane (**6**) to **4** is highly aromatic. For example, the C—C separations of the six active carbon centers are typical of delocalized systems. The calculated Λ of -38.9 ppm cgs (relative to the increment value for **6**) and the calculated NICS value of -26.8 ppm at the geometric center of the six-carbon delocalized system indicate the aromatic character. These values are in sharp contrast to those for **4**.

Furthermore, diademane (**6**) also has a larger χ_{tot} than
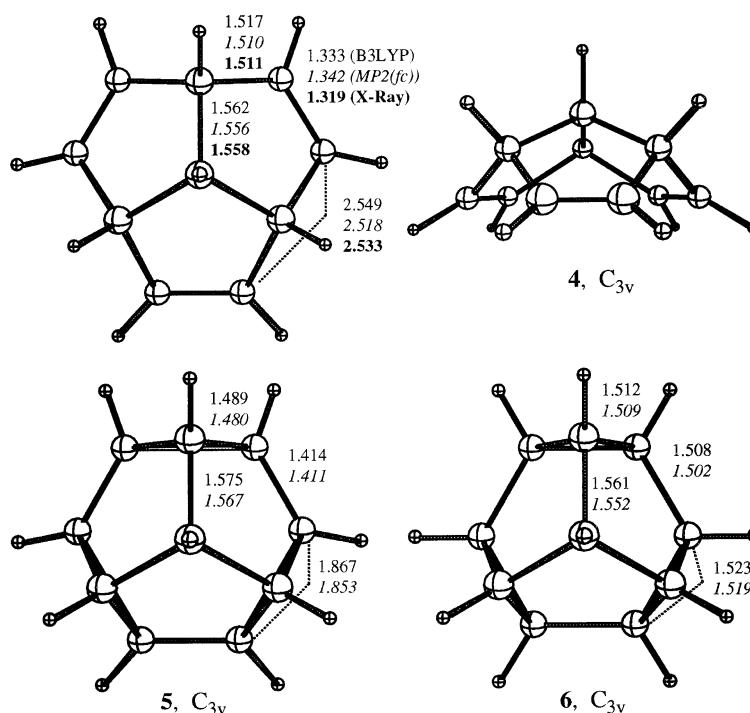
Figure 4. Optimized geometries for triquinacene (**4**), the cyclization transition state (**5**) and diademane (**6**)

Table 2. Computed total energies (au), *ZPE* (kcal mol^{-1}) and relative energies (kcal mol^{-1}), magnetic susceptibilities (χ_{tot}), magnetic susceptibility enhancements (Λ, ppm cgs) and NICS values for the isomerization of triquinacene (**4**) to diademane (**6**)

Parameter	**6**	**5** (TS)	**4**
HF/6–31G*	−384.39190	−384.30811	−384.45138
ZPE (NIMAG)[a]	103.2 (0)	100.7 (1)	102.4 (0)
MP2(fc)/6–31G*	−385.68285	−385.63584	−385.72275
E_{rel} (MP2)[b]	0.0	26.9	−25.8
B3LYP/6–311 + G**	−387.05977	−387.01507	−387.12025
E_{rel} (B3LYP)[c]	0.0	25.5	−38.8
χ(tot)[d]	−126.2	−153.9	−103.2
Λ	−11.2[e]	−38.9[f]	−0.2[g]
NICS[h]	−10.9	−26.8	−2.3

[a] At HF/6–31G*, scaled by 0.89.
[b] At MP2(fc)/6–31G* + *ZPE* (HF/6–31G*).
[c] At B3LYP/6–311 + G** + *ZPE* (HF/6–31G*).
[d] At IGLO/DZ//MP2/6–31G*.
[e] Relative to the >CH— group increment taken from Ref. 26.
[f] Relative to the increment for **6**.
[g] Relative to increment values of four >CH— and three *cis* —HC=CH— groups taken from Ref. 26.
[h] GIAO-SCF/6–31G*//MP2(fc)/6–31G* computation at the geometric center of the six active carbon atoms.

triquinacene (**4**). The difference between the calculated χ_{tot} of **6** and the increment value for 10 methine groups gives an estimated exaltation of −11.2 ppm cgs. We ascribe this to the contribution of the three-membered rings in **6**. Cyclopropane and substituted cyclopropanes

have been computed to have exaltations of *ca* −4.5 ppm.[26]

Consistent with the Woodward–Hoffmann rules, the thermal isomerization from diademane (**6**) to triquinacene (**4**) is a concerted process. The computed activation energies of 26.9 [MP2/6–31 + G* + *ZPE* (HF/6–31G*)] and 25.5 kcal mol^{-1} [B3LYP/6–311 + G** + *ZPE* (HF/6–31G*)] (Table 2) are 1.4 and 2.8 kcal mol^{-1} smaller than the experimental activation energy of 28.3 ± 0.1 kcal mol^{-1} in solution.[27]

Some typical pericyclic aromatic transition structures

In addition to the examples discussed above, we consider some of the typical aromatic transition structures of pericyclic reactions. Since the aromaticity of most of these transition states have been investigated extensively
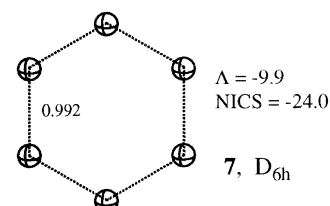
Figure 5. B3LYP/6–311 + G(D,3PD) H$_6$ (**7**, D_{6h}) and the calculated Λ (IGLO/II) and NICS values (SOS-DFPT-PW91/III)
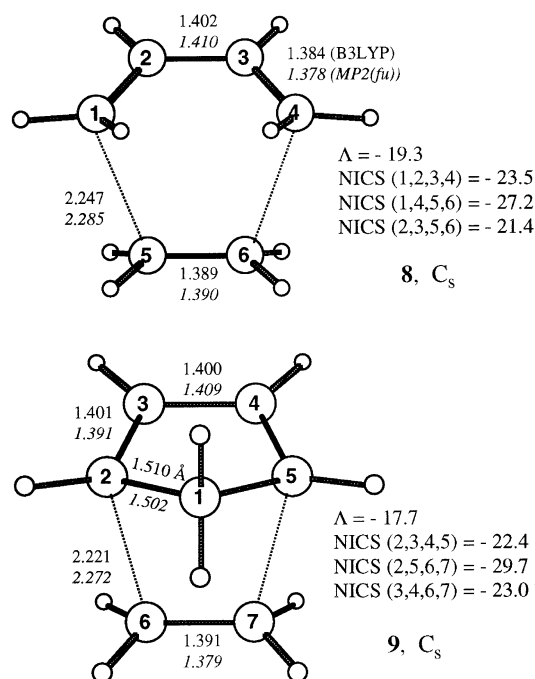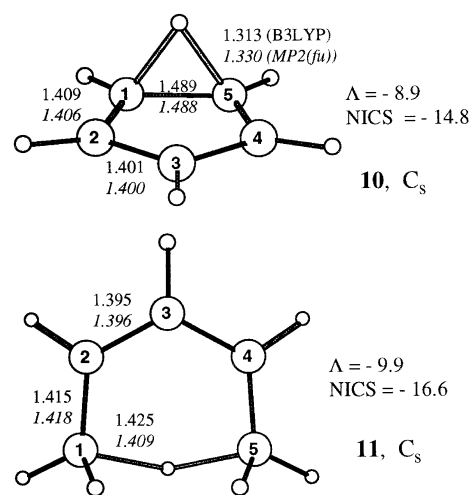
Figure 6. Optimized geometries for the transition state of the Diels–Alder reaction between ethylene and butadiene (**8**) and cyclopentadiene (**9**), and the calculated Λ (IGLO/II) and NICS values (GIAO-SCF/6–31G*//B3LYP/6–311 + G**)

Figure 7. Optimized geometries for the 1,5-H shift transition states in cyclopentadiene (**10**) and 1,3-pentadiene (**11**) and the calculated Λ (IGLO/II) and NICS values (GIAO-SCF/6–31G*//B3LYP/6–311 + G**)

on the basis of geometric, energetic and magnetic criteria,[8] we present here our new NICS analyses as additional information.

Aromaticity of the D_{6h} H$_6$ structure (7). The D_{6h} symmetrical H$_6$ structure (**7**) is an authentic transition state for the hydrogen exchange of three hydrogen molecules. The aromaticity of this σ-delocalized structure is evidenced by the large 'energy of concert' of *ca* 30 kcal mol^{-1} (the difference between the computed activation and the H—H bond dissociation energies). The Λ of D_{6h} H$_6$ is -9.4 ppm cgs (the benzene Λ is -13.4 ppm cgs).[28] Although our NICS value of -24.0 ppm is much larger than the NICS(tot) of benzene (-8.8), it is close to the benzene NICS(π) of -20.7. This indicates that the six delocalized σ-electrons in **7** are comparable to the six π-electron delocalization in benzene. Therefore, aromaticity is associated directly with cyclically delocalized electrons which can have σ, π or hybrid character.

Diels–Alder reactions between ethylene and butadiene and cyclopentadiene. As a pericyclic prototype, the Diels–Alder reaction of ethylene and butadiene has been studied at many computational levels. The concerted and synchronous mechanism with a C_s transition structure (**8**) is more favorable energetically by 2–7 kcal mol^{-1} than the stepwise alternative.[29] As shown in Fig. 6 bond length alternations in the diene moieties at B3LYP/6–311 + G** (0.018 Å for **8** and 0.001 Å for **9**)

are smaller than at MP2(fu)/6–31G* (0.042 Å for **8** and 0.018 Å for **9**). Evans' suggestion that **8** is aromatic was confirmed by the geometric, energetic and especially by our magnetic analysis based on the calculated ^{1}H NMR chemical shifts, magnetic susceptibility anisotropies and magnetic susceptibility enhancements.[8c] As further evidence, NICS points were calculated at various positions in **8**. For example, the NICS at the geometrical central point of the *cis*-butadiene moiety in **8** (C-1, -2, -3, -4) is -23.5 ppm and at the central point of orbital overlap area (C-1, -2, -5, -6) is -27.2 ppm. These large NICS values indicate the high aromaticity of the transition state. Similar results have been found for the aromatic transition state (**9**) involving ethylene and cyclopentadiene, e.g. NICS at the central point of the orbital overlap area (C-2, -5, -6, -7) is -29.7 ppm. Note that the NICS value at the center of the cyclopentadiene subunit of -22.4 is much larger in magnitude than that in cyclopentadiene itself (-4.2 ppm).

Transition states for 1,5-H shifts. The transition states of the degenerate 1,5-H shifts in cyclopentadiene (**10**) and in (*Z*)-1,3-pentadiene (**11**) have also been the subject of many theoretical calculations.[8d,30] The B3LYP/6–311 + G** geometries agree well with the MP2(fu)/6–31G* values (Fig. 7). Both **10** and **11** are highly aromatic based on the geometric, energetic and magnetic criteria.[8d] The NICS values (Fig. 7) at the geometrical centers of the five carbon atoms, -14.8 and -16.6 ppm, respectively, support the above conclusion. The former value is much more negative that the cyclopentadiene NICS (-4.2 ppm). We also have found that such degenerate reactions can be accelerated electrostatically by complexation with lithium and other metal cations.[8d] The aromaticity of these transition state complexes is evi-
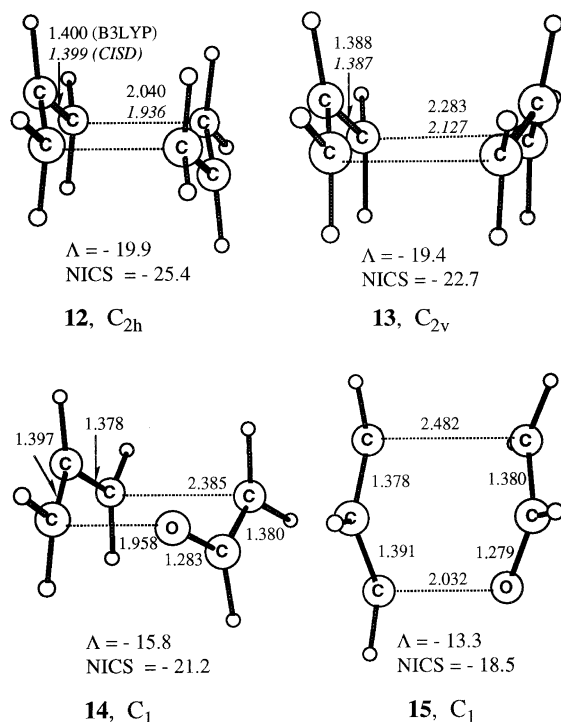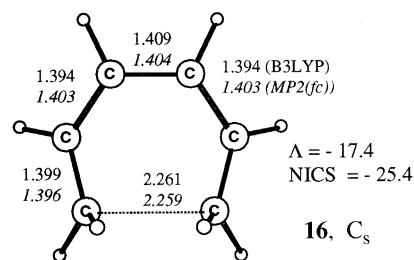
Figure 8. Optimized geometries for the transition states of Cope (**12, 13**) and Claisen (**14, 15**) rearrangements; the calculated Λs (IGLO/II//CISD for **12** and **13** and IGLO/DZ// B3LYP/6–311 + G** for **14** and **15**) and the NICS values (GIAO-SCF/6–31G*//B3LYP/6–311 + G**)

Figure 9. Optimized geometries for the transition state (**16**) of hexatriene ring closure and the calculated Λ (IGLO/II) and NICS values (GIAO-SCF/6–31G*//B3LYP/6–311 + G**)

denced by the calculated upfield Li^+ chemical shifts of -5.7 and -7.7 ppm, respectively.

Cope and Claisen rearrangements. The mechanism of the Cope rearrangement has been highly controversial.[7b,c,31] Which is the pathway? Does this reaction have a stepwise mechanism via an intermediate or a concerted one-step reaction path? Does the transition state have diyl (singlet diradical) or aromatic character?[8f] The puzzle of the reaction mechanism was complicated by the inaccurate experimental reference data used to estimate the energy of the hypothetical 1,4-cyclohexanediyl. At first, this was found to be isoenergetic with the measured activation energy.[32] Later, using more refined experimental data, the 1,4-cyclohexanediyl was estimated to be 9 kcal mol^{-1} higher in energy than the transition state, and 'the archetypal Cope rearrangement' was restored 'securely to the land of concert.'[33]

Owing to the 'pathological' flat potential energy surface, most of the conventional computational methods do not reproduce the experimental results.[8f] For example, MP2 calculations predict a stepwise reaction path with a tight 1,4-diyl intermediate, but the very expensive CISD optimizations combined with QCISD(T) single-point energy estimation reproduce the experimental results excellently.[8f] In addition, the economic hybrid B3LYP method was shown to give results close to experi-

ment.[8f,34] The B3LYP/6–311 + G** geometries agree very well with the highly correlated CISD/6–31G* results (Fig. 8).

Since the Cope rearrangement is a concerted process, the transition state (**12**) should also be aromatic. This is indicated by our energetic, geometric and magnetic analysis.[8f] The concerted and synchronous transition state is more aromatic than the 'artificial' stepwise transition state or intermediate. The aromaticity is also indicated by our NICS values, not only for the chair (-25.4 ppm) but also for the boat (-22.7) transition structure (**13**).

The [3,3]sigmatropic rearrangement of allyl vinyl ether to form 4-pentenal, the Claisen rearrangement, is closely related to the Cope rearrangement. As reported by Houk and co-workers,[34] the B3LYP functional gives a geometry intermediate between HF and CASSCF(6,6), and reproduces the experimental activation energy well. In contrast to the Cope rearrangement, there are no prior magnetic analyses of the transition structures. Hence we now characterize the transition state on the basis of Λ and NICS. At GIAO-SCF/6–31G*, the computed NICS at the geometrical central point of the six heavy atoms is -21.2 ppm for the chair-like (**14**) and -18.5 ppm for the boat-like (**15**) transition structures; **14** is more aromatic than **15**. This conclusion is also supported by the calculated Λ values, e.g. -15.8 ppm cgs for **14** and -13.3 ppm cgs for **15**.

Ring closures of hexatriene. The disrotatory ring closure of 1,3,5-hexatriene to 1,3-cyclohexadiene has been investigated at various computational levels.[8e,35] As shown in Fig. 9 both B3LYP/6–311 + G** and MP2(fc)/ 6–31G* geometries agree well. The aromaticity of the transition state (**16**) of the hexatriene cyclization has been studied on the basis of geometric, energetic and especially on the magnetic criteria.[8e] For example, the magnetic susceptibility maximum along the reaction coordinate coincides with the energy of the transition state. The calculated Λ of -17.4 ppm, comparable to the benzene value (-13.4 ppm), indicates its aromatic character. We also found that this reaction can be accelerated considerably electrostatically by metal cation complexation.[8e] The calculated Li^+ chemical shift of

−7.8 ppm in the complexed transition state is another probe characterizing aromaticity. In addition, the NICS of −16.3 ppm computed at the center of the six-carbon atoms indicates the considerable aromaticity of the transition state.

Pericyclic reactions with Möbius transition states. In contrast to the Hückel aromatic transition states with $4n + 2$ electrons, thermally allowed transition structures with $4n$ delocalized electron are Möbius aromatics.[4,5] The first example subjected to our energetic, geometric and magnetic analysis was the transition state (**17**) of the 1,7-H shift in 1,3,5-heptatriene with eight delocalized electrons.[8a] The strongly delocalized structure (B3LYP/ 6–311 + G** and MP2(fu)/6–31G*) of **17** is shown in Fig. 10. We not only found the strongly equalized bond lengths in **17**, but also a large energy of concert of *ca* 60 kcal mol^{-1} and a significant Λ of −23.1 ppm cgs. All these data show the transition state to be aromatic. In addition, the calculated ^{1}H NMR chemical shifts, especially for the two different methylene protons at C-1 and C-7, are revealing. The equatorial protons are computed to have $\delta = 5.6$ ppm, but the axial protons which point toward to the ring center are strongly shifted

upfield by −4.6 ppm owing to the strong ring current effects. As expected, the other C—H equatorial protons are shifted downfield by 8.1–9.0 ppm. The Möbius aromaticity of this transition structure is also evidenced by the calculated NICS of −14.0 ppm at the geometrical center of the seven carbon atoms.

Our second Möbius aromatic example is the ring closure transition state (**18**) of 1,3,5,7-octatetraene, which has eight delocalized electrons. However, the geometry of **18** depends strongly on the computational methods used.[8b] For example, the C-1—C-8 distance is 2.200 Å at HF/6–31G* but 2.511 Å at MP2/6–31G* and 2.420 Å at BLYP/6–31G*. The bond length alternation at MP2/6–31G* of 0.072 Å is much larger than that of 0.034 Å at HF/6–31G*. On this basis, **18** is more aromatic at HF/6–31G* than at MP2/6–31G*. The same conclusion can also be deduced from the calculated Λ, i.e. −12.6 ppm cgs for the MP2 and −28.4 ppm cgs for the HF geometry. This indicates that electron correlation favors a more localized transition state geometry, contrary to the general experience. Using another electron correlation approach, we re-optimized the transition structure at B3LYP/6–311 + G**; the C-1—C-8 distance of 2.313 Å is shorter than 2.511 Å at MP2 and the other C—C bond lengths are close to the HF/6–31G* values. In addition to our previous geometric, energetic and magnetic analyses,[8b] we calculated the NICS values at the eight-carbon central point: NICS is −6.6 for the MP2/6–31G*, −12.0 for the B3LYP/311 + G** and −13.2 ppm for the HF/6–31G* geometries. These indicate again that the HF/6–31G* transition state is more aromatic than that at MP2/6–31G*.

The third example of a Möbius aromatic transition state (**19**) involves the ring opening of cyclobutene to butadiene. This conrotatory electrocyclic reaction has been studied extensively at various *ab initio*[36] and DFT levels.[35] There are four delocalized electrons in this transition state. As pointed by Houk and co-workers,[35] the geometry of the transition structure hardly depends on the computational method used, but only correlated levels with large basis sets reproduce the known thermochemistry. The aromaticity of this transition state is indicated by the calculated NICS of −12.3 ppm at the four-carbon center as compared with that (0.0 ppm) at the center of cyclobutene and by the Λ of −5.2 ppm cgs relative to cyclobutene.

In conclusion, we have characterized the aromaticity of the pericyclic transition states based on the geometric, energetic and especially the magnetic criteria. Such transition states have not only delocalized structures and large energies of concert, but also significant magnetic susceptibility enhancements (Λ) and large NICS values On this basis, aromaticity is directly associated with cyclic electron (σ, π and hybrid character) delocalization. In agreement with the energetic analysis, both Λ (−0.2 ppm cgs) and NICS (−2.3 ppm) show that triquinacene is not homoaromatic. The magnetic criteria
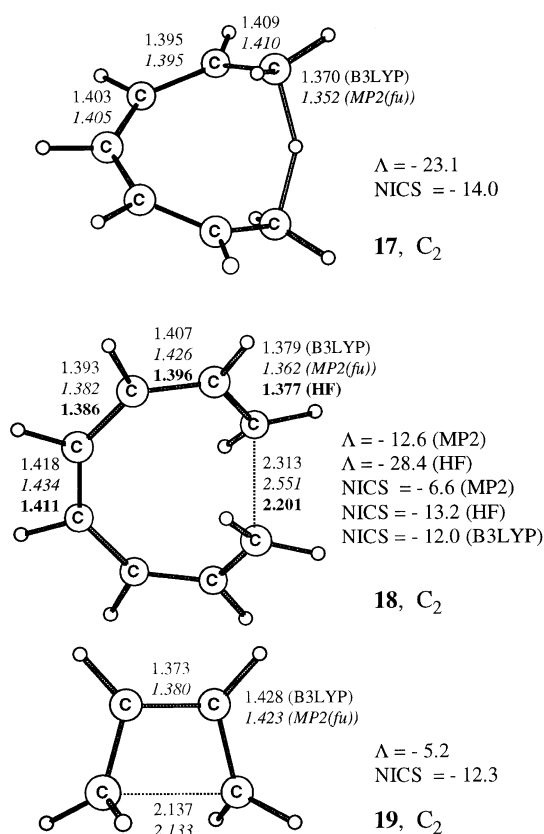
Figure 10. Optimized Möbius transition structures of the 1,7-H shift in 1,3,5-heptatriene (**17**), the ring closure of 1,3,5,7-octatetraene (**18**) and the ring opening of cyclobutene (**19**) and the calculated Λ (IGLO/II) and NICS values (GIAO-SCF/6–31G*//B3LYP/6–311 + G**)

of aromaticity are simpler to employ and often less arbitrary than the geometric and energetic criteria.

Acknowledgments

REFERENCES

1. M. G. Evans and E. Warhurst. *Trans. Faraday Soc.* **34,** 614 (1938).
2. M. G. Evans. *Trans. Faraday Soc.* **35,** 824 (1939).
3. R. B. Woodward and R. Hoffmann. *The Conservation of Orbital Symmetry.* Verlag Chemie, Weinheim (1970).
4. H. Zimmerman. *Acc. Chem. Res.* **33,** 272 (1971).
5. . For a review see M. J. S. Dewar. *Angew. Chem., Int. Ed. Engl.* **10,** 761 (1971), and references cited therein.
6. M. J. S. Dewar and C. Jie. *Acc. Chem. Res.* **25,** 537 (1992), and references cited therein.
7. . For review see (a) K. N. Houk, Y. Li and J. D. Evanseck. *Angew. Chem., Int. Ed. Eng.* **31,** 682 (1992); (b) K. N. Houk, J. Gonzalez and Y. Li. *Acc. Chem. Res.* **28,** 81 (1995); (c) W. T. Borden. *Acc. Chem. Res.* **29,** (1996); (d) W. R. Dolbier, Jr, H. Koroniak, K. N. Houk and C. Sheu. *Acc. Chem. Res.* **29,** 471 (1996); (e) J. J. Gajewski. *Acc. Chem. Res.* **30,** 219 (1997); (f) J. Bertran, V. Branchadell, A. Oliva and M. Sodupe. *Acc. Chem. Res.* in press.
8. (a) H. Jiao and P. v. R. Schleyer. *Angew. Chem., Int. Ed. Engl.* **32,** 1763 (1993); (b) H. Jiao and P. v. R. Schleyer. *J. Chem. Soc., Perkin Trans. 2* 407 (1994); (c) R. Herges, H. Jiao and P. v. R. Schleyer. *Angew. Chem., Int. Ed. Engl.* **33,** 1376 (1994); (d) H. Jiao and P. v. R. Schleyer. *J. Chem. Soc., Faraday Trans.* **90,** 1559 (1994); (e) H. Jiao and P. v. R. Schleyer. *J. Am. Chem. Soc.* **117,** 11529 (1995); (f) H. Jiao and P. v. R. Schleyer. *Angew. Chem., Int. Ed. Engl.* **34,** 334 (1994).
9. For a review see O. Wiest and K. N. Houk. *Top. Curr. Chem.* **182,** 1 (1996).
10. W. v. E. Doering, W. R. Roth, R. Breuckman, L. Figge, H.-W. Lenartz, W. D. Fessner and H. Prinzbach. *Chem. Ber.* **121,** 1 (1988).
11. P. v. R. Schleyer, C. Maerker, A. Dransfeld, H. Jiao and N. J. v. E. Hommes. *J. Am. Chem. Soc.* **118,** 6317 (1996).
12. (a) H. Jiao and P. v. R. Schleyer. *Angew. Chem., Int. Ed. Engl.* **35,** 2383 (1996); (b) G. Subramanian, P. v. R. Schleyer and H. Jiao. *Angew. Chem., Int. Ed. Engl.* **35** 2638 (1996); (c) G. Subramanian, P. v. R. Schleyer and H. Jiao. *Organometallics* **16,** 2362 (1997); (d) H. Jiao, P. v. R. Schleyer, Y. Mo, M. A. McAllister and T. T. Tidwell. *J. Am. Chem. Soc.* **119,** 6561 (1997).
13. B. Lecea, I. Morao and F. Cossio. *J. Org. Chem.* **62,** 7033 (1997).
14. M. J. Frisch, G. W. Trucks, H. B. Schlegel, P. M. W. Gill, B. G. Johnson, M. A. Robb, J. R. Cheeseman, T. Keith, G. A. Petersson, J. A. Montgomery, K. Raghavachari, M. A. Al-Laham, V. G. Zakrzewski, J. V. Ortiz, J. B. Foresman, J. Cioslowski, B. B. Stefanov, A. Nanayakkara, M. Challacombe, C. Y. Peng, P. Y. Ayala, W. Chen, M. W. Wong, J. L. Andres, E. S. Replogle, R. Gomperts, R. L. Martin, D. J. Fox, J. S. Binkley, D. J. Defrees, J. Baker, J. P. Stewart, M. Head-Gordon, C. Gonzalez and J. A. Pople. *Gaussian 94, Revision D.3.* Gaussian, Pittsburgh, PA (1995).
15. (a) W. Kutzelnigg, M. Schindler and Fleischer. *NMR, Basic Principles and Progress.* Springer, Berlin (1990); (b) M. Schindler and W. Kutzelnigg. *J. Chem. Phys.* **76,** 1919 (1982).
16. J. Pipek and P. G. Mezey. *J. Chem. Phys.* **90,** 4916 (1989); for applications, see P. v. R. Schleyer, H. Jiao, N. J. R. van E. Hommes, V. G. Malkin and O. L. Markin. *J. Am. Chem. Soc.* **119,** 12669 (1997).
17. (a) V. G. Malkin, O. L. Malkin, L. A. Eriksson and D. R. Salahub. in *Modern Density Functional Theory,* edited by J. M. Seminario and P. Politzer, p. 273, and references cited therein. Elsevier, Amsterdam (1995), (b) V. G. Malkin, O. L. Malkin, L. A. Eriksson and D. R. Salahub. *J. Am. Chem. Soc.* **116,** 5898 (1994).
18. K. N. Houk, R. W. Gandour, R. W. Strozier, N. G. Rondan and L. A. Paquette. *J. Am. Chem. Soc.* **101,** 6797 (1979).
19. R. D. Bach, G. J. Wolber and H. B. Schlegel. *J. Am. Chem. Soc.* **107,** 2837 (1985).
20. (a) H. P. Dauben, Jr, J. D. Wilson and J. L. Laity. *J. Am. Chem. Soc.* **90,** 811 (1968); (b) H. P. Dauben, J. D. Wilson, Jr and J. L. Laity. *J. Am. Chem. Soc.* **91,** 1991 (1969); (c) H. P. Dauben, Jr, J. D. Wilson and J. L. Laity. in *Nonbenzenoid Aromatics,* edited by Synder, Vol. II. Academic Press, New York (1971).
21. P. v. R. Schleyer and H. Jiao. *Pure Appl. Chem.* **68,** 209 (1996); (b) P. v. R. Schleyer, P. Freeman, H. Jiao and B. Goldfuss. *Angew. Chem., Int. Ed. Engl.* **34,** 337 (1995); (c) H. M. Sulzbach, P. v. R. Schleyer, H. Jiao, Y. Xie and H. F. Schaefer III. *J. Am. Chem. Soc.* **117,** 1367 (1995); (d) P. v. R. Schleyer, H. Jiao, M. H. Sulzbach and H. F. Schaefer III. *J. Am. Chem. Soc.* **118,** 2093 (1996); (e) H. Jiao, N. J. R. van E. Hommes, P. v. R. Schleyer and A. de Meijere. *J. Org. Chem.* **61,** 2828 (1996); (f) T. Zywietz, H. Jiao, P. v. R. Schleyer and A. de Meijere, *J. Org. Chem.*, **63,** 3417 (1998); (g) M. Nendel, K. N. Houk, L. M. Tolbert, E. Vogel, H. Jiao and P. v. R. Schleyer, *J. Phys. Chem.* (1998) in press.
22. R. B. Woodward, T. Fukunaga and R. C. Kelly. *J. Am. Chem. Soc.* **86,** 3162 (1964).
23. E. D. Stevens, J. D. Kramer and L. A. Paquette. *J. Org. Chem.* **41,** 2267 (1976).
24. (a) J. F. Liebman, L. A. Paquette, J. R. Peterson and D. W. Rogers. *J. Am. Chem. Soc.* **108,** 8267 (1986); (b) D. W. Rogers, S. A. Loggins, D. D. Samuel and M. A. Finnerty. *Struct. Chem.* **1,** 481 (1990).
25. (a) M. A. Miller, J. M. Schulman and R. L. Disch. *J. Am. Chem. Soc.* **110,** 7681 (1988); (b) M. J. S. Dewar and A. J. Holder. *J. Am. Chem. Soc.* **111,** 5384 (1989); (c) J. W. Storer and K. N. Houk. *J. Am. Chem. Soc.* **114,** 1165 (1992); (d) S. P. Verevkin, H.-D. Beckhaus, C. Rückhardt, R. Haag, S. I. Kozhushkov, T. Zywietz, A. de Meijere, H. Jiao and P. v. R. Schleyer, *J. Am. Chem. Soc.* (1998) in press.
26. H. Jiao, R. Nagelskerke, H. A. Kurtz, R. V. Williams, W. T. Borden and P. v. R. Schleyer. *J. Am. Chem. Soc.* **119,** 5921 (1997); the IGLO/DZ magnetic susceptibility increment values (in ppm cgs) are -17.8 (Me), -14.8 ($>CH_2$), -11.5 ($>CH\!-\!$), -7.6 ($>C<$), -10.0 ($-CH=$), -6.9 ($>C=$) and -19.0 (*cis* $-HC=CH-$).
27. A. de Meijere, D. Kaufmann and O. Schallner, *Tetrahedron Lett.* 553 (1973).
28. H. Jiao, P. v. R. Schleyer and M. N. Glukhovtsev. *J. Phys. Chem.* **100,** 12299 (1996), and references cited therein.
29. (a) F. Bernardi, A. Bottoni, M. J. Field, M. F. Guest, I. H. Hillier, M. A. Robb and A. Venturini. *J. Am. Chem. Soc.* **110,** 7478 (1988); (b) Y. Li and K. N. Houk. *J. Am. Chem. Soc.* **115,** 7478 (1993); (c) E. Goldstein, B. Beno and K. N. Houk. *J. Am. Chem. Soc.* **118,** 6036 (1996); (d) B. Beno, K. N. Houk and D. A. Singleton. *J. Am. Chem. Soc.* **118,** 9984 (1996).
30. F. Jensen and K. N. Houk. *J. Am. Chem. Soc.* **109,** 3139 (1987), and references cited therein.
31. D. A. Hrovat, K. Morokuma and W. T. Borden. *J. Am. Chem. Soc.* **116,** 1072 (1994).
32. W. v. E. Doering, V. G. Toscano and G. H. Beasley. *Tetrahedron,* **27,** 5299 (1971).
33. W. R. Roth, H.-W. Lenartz, W. v. E. Doering, L. Birladeanu, C. Guyton and T. Kitagawa. *J. Am. Chem. Soc.* **112,** 1722 (1990).
34. (a) O. Wiest, K. A. Black and K. N. Houk. *J. Am. Chem. Soc.* **116,** 10336 (1994); (b) H. Y. Yoo and K. N. Houk. *J. Am. Chem. Soc.* **116,** 12047 (1994), and references cited therein.
35. O. Wiest, K. N. Houk, K. A. Black and B. Thomas IV. *J. Am. Chem. Soc.* **117,** 8594 (1995).
36. D. C. Spellmeyer and K. N. Houk. *J. Am. Chem. Soc.* **110,** 3412 (1988), and references cited therein.